Isı Bilimi ve Tekniği Dergisi, 31,2, 13-24, 2011
J. of Thermal Science and Technology

ISSN 1300-3615

THREE-DIMENSIONAL NUMERICAL ANALYSIS OF FORCED CONVECTION FLOW AND HEAT TRANSFER IN A CURVED SQUARE DUCT

Nevzat ONUR, Oğuz TURGUT ve Kamil ARSLAN
Gazi University, Faculty of Engineering, Department of Mechanical Engineering
06570, Maltepe, Ankara, Turkey
nevonur@gazi.edu.tr , oturgut@gazi.edu.tr , kamilarslan@gazi.edu.tr

(Geliş Tarihi: 09.12. 2009, Kabul Tarihi: 01.07.2010)

Abstract: A three-dimensional numerical study of a constant property Newtonian fluid in 90^o strongly curved duct having a constant square cross section under steady and laminar flow conditions is presented for a uniform wall temperature boundary condition. Numerical solutions were obtained using commercial software Ansys Fluent 6.3.26 for the range of 165≤De≤1450 (250≤Re≤2200). The working fluid was air (Pr≅0.7). The average Nusselt numbers and average Darcy friction factors are obtained, which can be used in estimation of flow and heat transfer performance in curved duct. In addition, local Nusselt numbers, local Darcy friction factors, velocity magnitude and temperature profiles, and secondary velocities are analyzed. Results are compared with the literature for validation of the numerical approach. It is seen that present results are in good agreement with the literature results.

Keywords: Laminar flow, Curved square duct, Forced convection, Heat transfer, Ansys Fluent

BİR EĞRİSEL KARE KANAL İÇERİSİNDEKİ ZORLANMIŞ KONVEKSİYON AKIŞ VE ISI TRANSFERİNİN ÜÇ BOYUTLU SAYISAL ANALİZİ

Özet: Kararlı ve laminer akış şartlarında sabit kare kesit alanına sahip 90^o'lik fazlasıyla eğrisel kanal içerisindeki sabit özellikli Newtonsel akışkanın üç boyutlu sayısal analizi üniform duvar sıcaklığı sınır şartı için sunulmuştur. Sayısal sonuçlar 165≤De≤1450 (250≤Re≤2200) değerleri için elde edilmiştir. Akışkan olarak hava (Pr≅0.7) kullanılmıştır. Eğrisel kanal içerisindeki akış ve ısı transferi performansının tahmininde kullanılabilen ortalama Nusselt sayıları ve ortalama Darcy sürtünme faktörleri elde edilmiştir. Buna ilaveten yerel Nusselt sayıları, yerel Darcy sürtünme faktörleri, hız büyüklük ve sıcaklık profilleri, ve ikincil hızlar analiz edilmiştir. Sonuçlar sayısal yaklaşımın geçerliliği için literatür ile kıyaslanmıştır. Mevcut sonuçların literatür sonuçlar ile uyum içerisinde olduğu görülmüştür.

Anahtar Kelimeler: Laminer akış, Eğrisel kare kanal, Zorlanmış taşınım, Isı transferi, Ansys Fluent

INTRODUCTION

Curved ducts of various cross sections are used widely in many industrial devices such as the passages of turbomachinery components, inlet diffusers of rocket engines, heat exchangers, cooling systems, refrigeration and air conditioning systems. Flow in curved tubes is different from flow in straight ducts. The main future of the flow in curved ducts is the presence of the secondary flow produced by the centrifugal force of the axial flow and the curvature effect. This secondary flow motion causes an increase in the heat transfer. It also causes serious pressure drop in curved ducts. A through understanding of the heat flux and the wall shear stress at curved duct wall is very important in order to analyze and design thermal equipment such as heat exchangers.

In consideration of the wide range of applications in engineering, flow and heat transfer in curved ducts have been studied extensively in the literature for different curved shapes. Review articles on steady fully developed flow are available by Berger et al. (1983), Ito (1987), and Naphon and Wongwises (2006).

For square cross section, which is the principal interest of the present work, Mori et al. (1971) presented numerical and experimental results for fully developed laminar flow in a 220^o curved channel with a square cross section under uniform heat flux, using a boundary layer approximation. Cheng et al. (1975) numerically investigated thermal entrance region heat transfer in curved square channels for constant wall temperature

and uniform wall heat flux conditions. Humphrey et al. (1977) experimentally and numerically investigated laminar flow in a 90^o bend, 40 x 40 mm cross section, of strong curvature using water as the working fluid in the channel. Calculated values of the three velocity components and measured values of the longitudinal component were reported. The experiments were conducted at a Dean number of 368 (corresponding to a Reynolds number of 790). 90^o bend is attached to the end of the 1.8 m rectangular channel. In addition, the bend was located in the vertical plane with a 1.2 m length of straight duct of the same cross section attached to its downstream end. Ye et al. (1980) numerically investigated the heat transfer for developing steady laminar flow of a nonbuoyant incompressible fluid in 90^o strongly curved ducts for the aspect ratio of 1/3, 1 and 3. Study was carried out for two Dean numbers 368 and 260, and two different curvature ratios 2.3 and 4.6. Chilukuri and Humphrey (1981) studied numerically developing heat transfer in a 90^o strongly curved square duct using a finite-difference method for the steady state, constant wall temperature boundary condition and incompressible laminar flow of a constant property fluid. The influence of buoyancy force was included in the computations. Hille et al. (1985) examined the development of laminar flow in a 180^o section of a curved square duct having curvature ratio of 6.45. Winters (1987) numerically carried out steady, fully developed laminar flow in a curved square and rectangular cross-section. Soh (1988) numerically studied the developing steady laminar flow in a curved duct of square cross-section for the Reynolds number of 574 and 790 and curvature ratios of 6.45 and 2.3. Hwang and Chao (1991) studied numerically the laminar forced convection in a curved isothermal square duct for hydrodynamically and thermally fully developed conditions using a finite-difference implicit-scheme approximation for large dimensionless radii of curvature. The range of Dean number is between 0 and $1x10^3$. The Prandtl number of the fluid was 0.7 and 7. Bara et al. (1992) carried out an experimental and numerical study of the flow development and fully developed flows of an incompressible Newtonian fluid in a curved square cross section with a curvature ratio of 15.1. Results are obtained for three Dean numbers 125, 137, and 150. Chung and Hyun (1992) presented a numerical study of developing laminar flow in 90^o curved square duct with strong curvature over wide ranges of Reynolds numbers under constant wall temperature and constant wall heat flux boundary conditions. Straight inlet and outlet tangents were attached to the duct. Average pressure coeffients and average Nusselt numbers at various positions were given. Silva et al. (1999) numerically examined the laminar flow in curved ducts with elliptic or rectangular cross section with aspect ratios between 0.7 and 1.4 for steady, incompressible and fully developed flow under constant wall temperature boundary condition. Yanase et al. (2002) investigated the steady laminar flow in a curved rectangular duct for a range of the aspect ratio between 1 and 12 using the spectral method. Papadopoulos and Hatzikonstantinou (2004) numerically investigated the laminar fully developed flow in curved square ducts with internal fins using the SIMPLE algorithm. Papadopoulos and Hatzikonstantinou (2005) studied the laminar incompressible hydrodynamically fully developed and thermally developing flow in a curved square duct with internal fins.

It can be concluded from the survey of the existing literature that data on the three-dimensional fluid flow in a strongly curved duct with a square cross section is limited. The purpose of this work is to investigate numerically the three-dimensional laminar flow heat transfer in a 90^o strongly curved duct having a square cross section for a uniform wall temperature boundary condition. At the inlet of the curved duct, a parabolic velocity profile is imposed. Air ($Pr \cong 0.7$) is used as the working fluid. The effects of secondary flows on fluid flow and convective heat transfer are investigated by calculation of local and average Darcy friction factor and Nusselt number for a wide range of Dean numbers. Flow characteristics are also presented. This study is motivated by the fact that reliable numerical simulation is a fast and inexpensive good compliment of expensive and time consuming experimental work.

DESCRIPTION OF THE PHYSICAL PROBLEM

The geometry and characteristics of the curved channel with square cross section used in the present study are shown in Figure 1. The side length of the cross section is denoted by 2a, 100 mm. In other words, the duct aspect ratio is unity. In Figure 1, R_c designates the radius of curvature and its value is 230 mm. Hence, curvature ratio, $R_c/2a$, is 2.3 in this study.

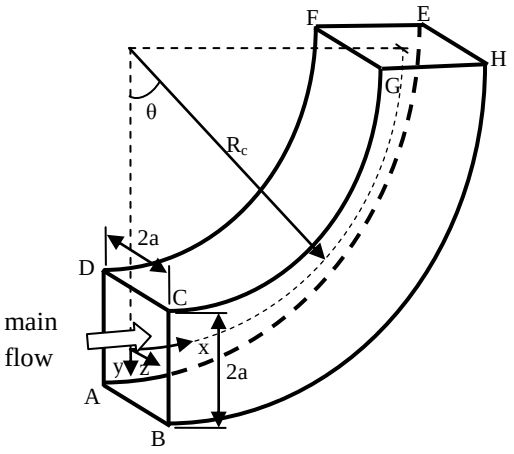

Figure 1. Flow geometry and computational domain

MATHEMATICAL MODEL

The steady laminar flow in the curved duct is considered. All the thermophysical properties are assumed to be constant. Air is considered to be an incompressible Newtonian fluid. Viscous dissipation and radiative transport are considered to be negligibly

small and dropped from the energy equation. A uniform wall temperature boundary condition is considered for the curved duct.

Coordinate system is shown in Figure 1. In this system, the radius of curvature of the duct axis is shown by R_c. The distance along the duct axis is shown by x, the distance in the radial direction measured from the duct axis by y, and the transverse distance from the duct axis is given by z. The velocity components in the directions of increasing x, y, z are u, v, w, respectively.

On the basis of the simplifying assumptions, the three-dimensional governing equations are summarized as follows (Ward-Smith, 1980; Hwang and Chao, 1991; Papadopoulos and Hatzikonstantinou, 2005)

Conservation of mass:

$$\frac{R_c}{(R_c+y)}\frac{\partial u}{\partial x}+\frac{\partial v}{\partial y}+\frac{\partial w}{\partial z}+\frac{v}{(R_c+y)}=0 \tag{1}$$

Conservation of momentum:

$$\frac{R_c}{(R_c+y)}u\frac{\partial u}{\partial x}+v\frac{\partial u}{\partial y}+w\frac{\partial u}{\partial z}+\frac{uv}{R_c+y}=$$
$$\frac{1}{\rho}\left[\frac{R_c}{R_c+y}\left(-\frac{\partial P}{\partial x}\right)+\mu\left\{\frac{R_c^2}{(R_c+y)}\frac{\partial^2 u}{\partial x^2}+\frac{\partial^2 u}{\partial y^2}+\frac{\partial^2 u}{\partial z^2}\right.\right. \tag{2a}$$
$$\left.\left.+\frac{1}{(R_c+y)}\frac{\partial u}{\partial y}+\frac{2R_c}{(R_c+y)^2}\frac{\partial v}{\partial x}-\frac{u}{(R_c+y)^2}\right\}\right]$$

$$\frac{R_c}{(R_c+y)}u\frac{\partial v}{\partial x}+v\frac{\partial v}{\partial y}+w\frac{\partial v}{\partial z}-\frac{u^2}{(R_c+y)}=$$
$$\frac{1}{\rho}\left[\left(-\frac{\partial P}{\partial y}\right)+\mu\left\{\left(\frac{R_c}{R_c+y}\right)^2\frac{\partial^2 v}{\partial x^2}+\frac{\partial^2 v}{\partial y^2}+\frac{\partial^2 v}{\partial z^2}\right.\right. \tag{2b}$$
$$\left.\left.+\frac{1}{R_c+y}\left[\frac{\partial v}{\partial y}-\frac{2R_c}{R_c+y}\frac{\partial u}{\partial x}-\frac{v}{R_c+y}\right]\right\}\right]$$

$$\frac{R_c}{(R_c+y)}u\frac{\partial w}{\partial x}+v\frac{\partial w}{\partial y}+w\frac{\partial w}{\partial z}=\frac{1}{\rho}\left[-\frac{\partial P}{\partial z}\right.$$
$$\left.+\mu\left\{\left(\frac{R_c}{R_c+y}\right)^2\frac{\partial^2 w}{\partial x^2}+\frac{\partial^2 w}{\partial y^2}+\frac{\partial^2 w}{\partial z^2}+\frac{1}{R_c+y}\frac{\partial w}{\partial y}\right\}\right] \tag{2c}$$

Conservation of energy:

$$\frac{R_c}{R_c+y}u\frac{\partial T}{\partial x}+v\frac{\partial T}{\partial y}+w\frac{\partial T}{\partial z}=$$
$$\alpha\left[\frac{{R_c}^2}{(R_c+y)^2}\frac{\partial^2 T}{\partial x^2}+\frac{\partial^2 T}{\partial y^2}+\frac{\partial^2 T}{\partial z^2}+\frac{1}{R_c+y}\frac{\partial T}{\partial y}\right] \tag{3}$$

where P, ρ, μ, and α are the fluid pressure (Pa), density (kgm^{-3}), dynamic viscosity ($kgm^{-1}s^{-1}$), and thermal diffusivity (m^2s^{-1}), respectively. The governing equations (1) through (3) have been applied in the computational domain of the physical model shown in Figure 1.

The physically realistic boundary conditions for the problem under consideration are discussed next. The application of the appropriate boundary conditions on the computational domain is crucial to carry out accurate simulations. EFGH face of the computational domain is the outlet and default pressure outlet boundary condition of the Ansys Fluent 6.3.26 was imposed on the exit of the computational domain. In case there is a reverse flow, its temperature is set to 298 K. ABCD face of the computational domain is the inlet. At the inlet of the curved pipe, a parabolic velocity profile is imposed. The imposed velocity profile is given as (Ward-Smith, 1980)

$$u(y,z)=-\frac{1}{2\mu}\frac{dp}{dx}\left[a^2-y^2\right.$$
$$\left.-\frac{4}{a}\sum_{n=0}^{\infty}\frac{(-1)^n}{{\beta_n}^3}\frac{\cosh(\beta_n z)}{\cosh(\beta_n a)}\cos(\beta_n y)\right] \tag{4}$$

where μ ($kgm^{-1}s^{-1}$) dynamic viscosity, a (m) half height of the cross section of the duct and $\beta_n=((2n+1)\pi)/2a$.

This eliminates the hydrodynamic entrance length required to obtain a fully developed velocity profile before heating begins. A user defined function (UDF) was written in order to impose this boundary condition. The temperature of the working fluid is set equal to 298 K at the inlet of the computational domain. Standard no slip boundary condition was used on the walls of the curved duct. A constant wall temperature boundary condition was imposed on the external walls of curved duct. The walls of the curved duct are kept at 313 K.

The most important overall flow and heat transfer characteristics of laminar forced convection in the three-dimensional duct for the design point of view are indicated by the average Nusselt number and average Darcy friction factor.

The characteristics of the flow in the curved duct can be represented by local and average Darcy friction factor as given below respectively (White, 2006)

$$f_x=8\bar{\tau}_{w,x}/\rho{u_m}^2 \tag{5}$$

$$f=8\bar{\tau}_w/\rho{u_m}^2 \tag{6}$$

where, $\bar{\tau}_{w,x}$ (Pa) is the peripherally averaged wall shear stress at x-position, $\bar{\tau}_w$ (Pa) is the average wall

shear stress on the channel, ρ (kgm^{-3}) is the density, and u_m (ms^{-1}) is the average axial velocity. Local wall shear stress can be obtained as below

$$\tau = \begin{cases} \mu\left(\frac{\partial u}{\partial y}\right) & \text{for horizontal-walls} \\ \mu\left(\frac{\partial u}{\partial z}\right) & \text{for vertical-walls} \end{cases} \quad (7)$$

The peripherally averaged wall shear stress can be expressed as:

$$\bar{\tau}_{w,x} = \frac{1}{4}\left[\int_A^B \tau dz + \int_B^C \tau dy + \int_C^D \tau dz + \int_D^A \tau dy\right] \quad (8)$$

The average wall shear stress on the channel can be calculated as:

$$\bar{\tau}_w = \int_{x=0}^{L} \bar{\tau}_{w,x} dx \Big/ \int_{x=0}^{L} dx \quad (9)$$

The average axial velocity u_m is given by (White, 2006)

$$u_m = \iint \rho u dA / \iint \rho dA \quad (10)$$

in which ρ (kgm^{-3}) and u (ms^{-1}) are the density and velocity respectively. Peripherally averaged local Nusselt number has been calculated from

$$Nu_x = \overline{q''_x} D_h / k\left(T_w - T_b\right)_x \quad (11)$$

where $\overline{q''_x}$ (Wm^{-2}) is the peripherally averaged heat flux at x-position, T_w and T_b (K) are the wall and average bulk temperatures at x-position. Local heat flux is calculated by

$$q'' = \begin{cases} -k\left(\frac{\partial T}{\partial y}\right) & \text{for horizontal-walls} \\ -k\left(\frac{\partial T}{\partial z}\right) & \text{for vertical-walls} \end{cases} \quad (12)$$

The peripherally averaged heat flux at x-position is determined by

$$\overline{q''_x} = \frac{1}{4}\left[\int_A^B q'' dz + \int_B^C q'' dy + \int_C^D q'' dz + \int_D^A q'' dy\right] \quad (13)$$

The average heat flux on the channel can be calculated as:

$$\overline{q''_w} = \int_{x=0}^{L} \overline{q''_x} dx \Big/ \int_{x=0}^{L} dx \quad (14)$$

The average bulk temperature T_b (K) is given by (White, 2006)

$$T_b = \iint \rho c_p u T dA / \iint \rho c_p u dA \quad (15)$$

where c_p ($Jkg^{-1}K^{-1}$) is the specific heat at constant pressure. The average Nusselt number for the duct is given as

$$Nu_m = h_m D_h / k = D_h \overline{q''_w} / k\left(T_w - T_m\right) \quad (16)$$

where D_h (m) is the hydraulic diameter defined as $D_h=4A/P$, with A (m^2) being the cross sectional area of the duct and P (m) is the wetted perimeter, h_m ($Wm^{-2}K^{-1}$) is the average heat transfer coefficient, k ($Wm^{-1}K^{-1}$) is the thermal conductivity, $\overline{q''_w}$ (Wm^{-2}) is the average heat flux, T_w (K) is the constant wall temperature, and T_m (K) is the average bulk temperature of the fluid and defined as

$$T_m = (T_{bi}+T_{bo})/2 \quad (17)$$

in which T_{bi} and T_{bo} (K) are the inlet and outlet bulk temperatures, respectively. Another important dimensionless quantity is the Reynolds number and it is defined as

$$Re = \rho u_m D_h / \mu \quad (18)$$

where ρ (kgm^{-3}) is the density of the fluid, u_m (ms^{-1}) is the average axial velocity, D_h (m) is the hydraulic diameter, and μ ($kgm^{-1}s^{-1}$) is the dynamic viscosity of the fluid. The Dean number is defined as

$$De = Re\,(D_h / R_c)^{1/2} \quad (19)$$

where D_h (m) is the hydraulic diameter and R_c (m) is the mean radius of curvature. Hence, Dean number used in this study ranges from 165 to 1450.

MESHING AND NUMERICAL SOLUTION

A numerical solution is carried out using commercial software Ansys Fluent 6.3.26 in order to understand the flow characteristics. The computational scheme used by Ansys Fluent Inc. is based on the finite volume discretization method. This method is described in detail by Patankar (1980) and Versteegh and Malalasekra (2007). The code provides mesh flexibility by structured and unstructured meshes.

Computations are performed for laminar flow conditions. The computational domain is depicted in Figure 1. Nonuniform hexahedral (structured) grids are employed for all numerical simulations performed in this work. In the present study, the structured hexahedral cells are created with fine mesh near the walls using mesh generation software Ansys Gambit 2.4.6. A dense grid distribution is employed near the

heat transfer wall while a uniform grid distribution is used in the flow direction. This is done to provide a sufficiently clustered mesh near the duct walls and to avoid sudden distortion and skewness. The flow gradients near the duct walls are expected to be large. The mesh characteristics are shown in Figure 2. The accuracy of the solution depends on the number and the size of the cells. The grid size used in computations is chosen by performing a grid independence study. Grid independence was achieved in this work according to the guidelines outlined by Freitas (1999). The grid independence study was conducted by altering the cell size inside the computational domain. Several meshes were tested to ensure that the solution was independent of the mesh. This test indicated that 25×25×90 cells for De=1450 are adequate. It is observed that further refinement of grids from 25×25×90 to 30×30×90 did not have a significant effect on the results in terms of average Nusselt number and average Darcy friction factor (less than 0.1%). Based on this observation, 25×25×90 cells were considered for the final simulation at De=1450. No convergence problems were observed. This grid is also used for other Dean numbers. Momentum relaxation factor in Ansys Fluent 6.3.26 was adjusted to obtain the proper convergence. Grid independence study makes one to utilize computational resources most efficiently as well as obtain reasonable results.

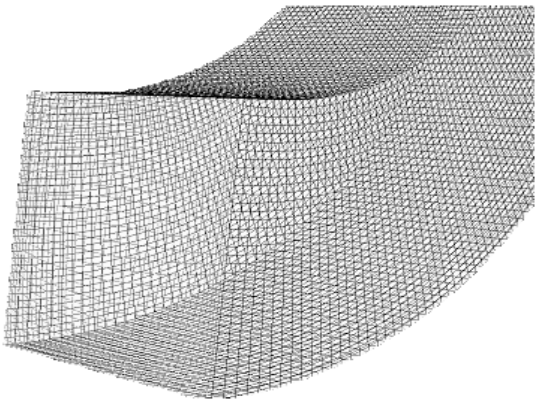

Figure 2. Mesh distribution in the computational domain

Steady segregated solver is adapted, which employs an implicit pressure-correction scheme (Ansys Fluent, 2006). The standard SIMPLE-algorithm has been used for pressure-velocity coupling. The second order upwind scheme is selected for spatial discretization of convective terms. Converged results are obtained after the residuals are smaller than the specified values. Converged results render mass residual of 10^{-5}, energy residual of 10^{-6} and momentum residual of 10^{-6}.

RESULTS AND DISCUSSION

The numerical computations were carried out for the curved duct having square cross section. The forced convection heat transfer in curved duct was investigated under laminar flow conditions. The Dean number De was varied in the range of 165 to 1450 (and corresponding to the Reynolds number from 250 to 2200). The air properties were evaluated at 298 K. The parametric study conducted produced a large number of results. In order to present some characteristic velocity and isotherm contours, some samples of results are chosen as shown below. All the figures are plotted on planes perpendicular to the main flow direction.

Figure 3a shows the typical velocity magnitude contours at the outlet plane of the duct for different Dean numbers. These velocity contours provide information on the effect of Dean numbers on the flow field. The convex surface of the duct influence flow more than the concave surface of the duct.

The typical temperature contours predicted by the present numerical computations for flow at the outlet plane of the duct are shown in Figure 3b for different Dean numbers. An inspection of these figures reveals the effect of Dean numbers on the heat transfer. A close study of these figures indicates that the centrifugal body forces have a strong influence on the heat transfer. At low Dean numbers the centrifugal body forces are weaker and the convective currents have strong influence on the flow. At higher Dean numbers the centrifugal body forces are now much stronger and the secondary flow motion begins to show its effect on flow and heat transfer. There are stronger temperature gradients on the convex surface of the duct. In other words, the convex surface of the duct influences heat transfer more than the concave surface of the duct. Figure 3a and 3b reveal that the flow development is symmetric about the vertical duct centerline (z=0).

The effect of curvature of the geometry on flow and heat transfer is investigated. Effect of curvature on flow velocity field is discussed first. For this purpose, the typical velocity magnitude contours predicted by the present numerical computations are plotted on planes created for 30^o, 60^o and 90^o for De=660. These results are depicted on Figure 4a. These contours indicate the fluid behaviour caused by the duct curvature which induces centrifugal body forces on the fluid. The effect of curvature on heat transfer is discussed next. For this purpose, the typical temperature contours predicted by the present numerical computations are plotted on planes created for 30^o, 60^o and 90^o for De=660 (see Figure 4b). An inspection of these figures reveals that the duct curvature has a strong influence on the flow and heat transfer. It is seen that the secondary flows resulting from centrifugal forces affect the distribution of the velocity and temperature. As can be seen in figure, the secondary flows resulting from centrifugal forces change the distribution of the flow.

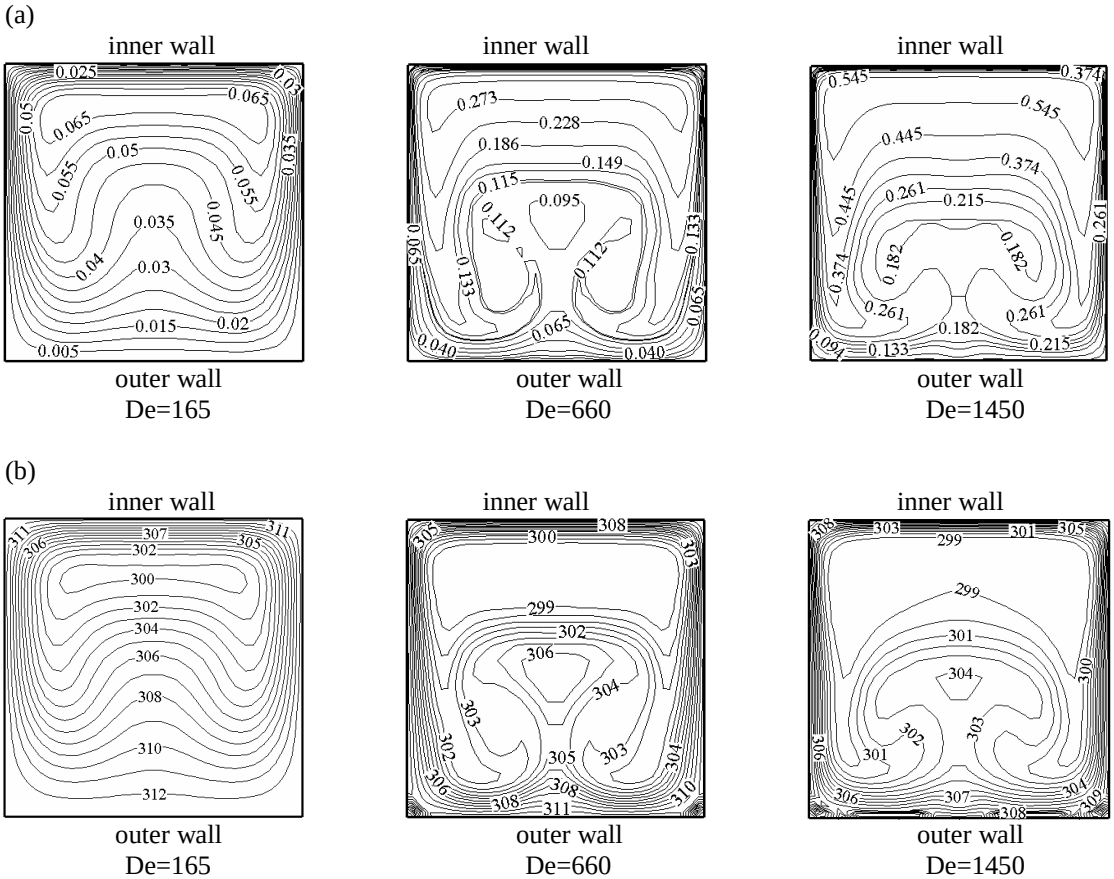

Figure 3. Contours on outlet plane for different Dean numbers (a) velocity magnitude, (b) temperature

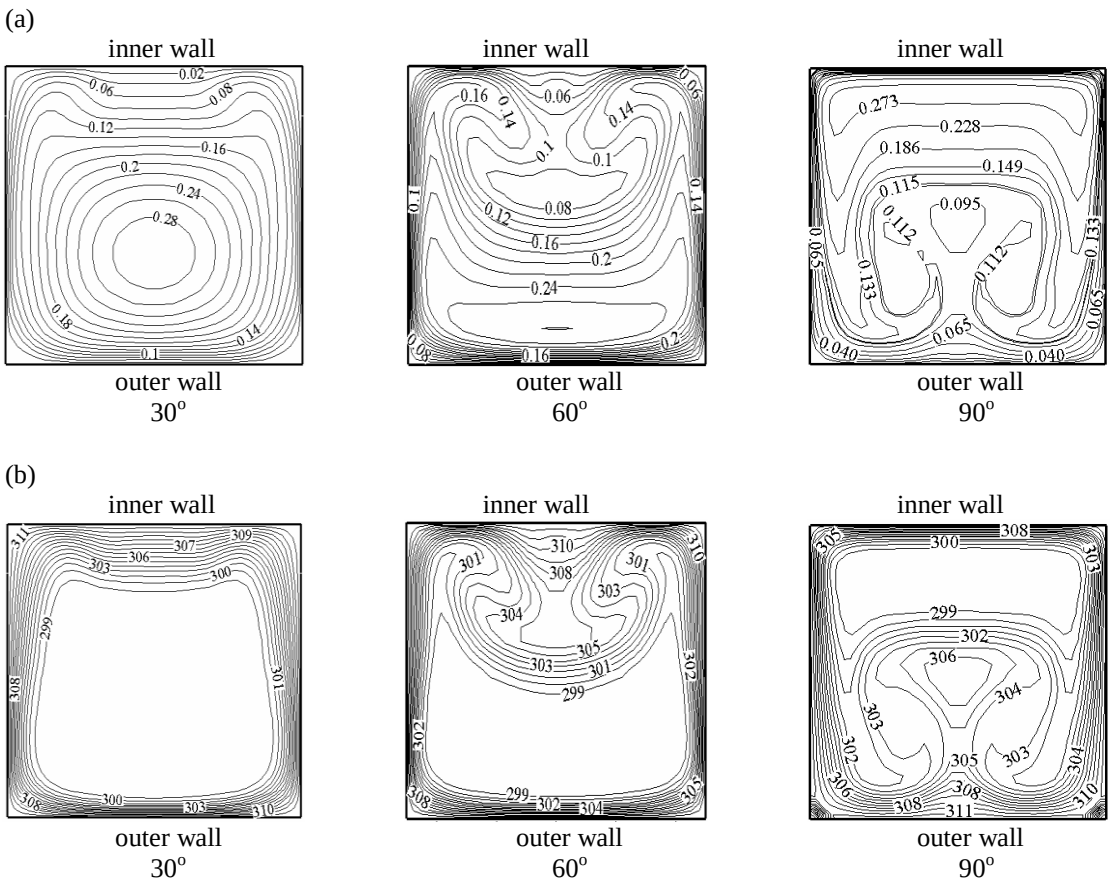

Figure 4. Contours for De=660 on planes created for different angles (a) velocity magnitude, (b) temperature

The typical secondary flow, $(v^2+w^2)^{0.5}$, contours on planes created for 15^o, 30^o, 45^o, 60^o, 75^o and 90^o for De=660 are shown in Figure 5. It is seen that as the flow enters the curved square duct a secondary flow develops immediately. As shown in Figure 5, the intensity of the secondary velocity increases up to 45^o. It is also seen that there are secondary velocities toward inner central region in the central outer wall. These secondary velocities push the vortex which is in the central region toward the inner wall up to 45^o and it disappears at 60^o. It is seen that additional secondary vortexes appear at 75^o. The formation of the additional vortexes is due to a centrifugal instability. It is also found that secondary velocities from central outer wall to the inner come to the middle of the channel at 75^o. At 90^o, additional vortex is seen near the central outer wall.

The typical secondary flow contours on plane created at 45^o for different Dean numbers are depicted in Figure 6. It is seen that the intensity of the secondary flow increases with the increase of the Dean number.

Typical secondary velocity vectors on the outlet plane are presented in Figure 7 for different Dean numbers. It is seen that the secondary flow occurs at the outlet plane because of the curvature of the duct. It can be seen that two main vortices form at the duct cross section as well. One of the main vortices is placed at the outer region rotating in the clockwise direction. In addition, the other main vortex are located at the inner region rotating in the counter-clockwise direction.

Figure 8a and 8b show the typical dimensionless axial velocity (u/u_m) along the channel at z = 0 and y = 0 symmetry planes, respectively, for value of De=660. In Figure 8a, the outer wall of the duct is at y/2a=0.5. It is seen that the maximum value of u/u_m shifts toward outer wall of the channel because of centrifugal force while θ increases. The phenomenon is similar to that observed by Soh (1988). As can be seen from Figure 8a, the maximum value of u/u_m increases with the increasing θ up to $\theta=75^o$. At the outlet of the channel the maximum value of u/u_m decreases. As for Figure 8b, it is seen that flow is symmetrical at z=0. As can be seen in Figure 8b, dimensionless velocity is parabolic at the beginning of the duct. In other words, flow is hydrodynamically fully developed at the duct inlet. However, hydrodynamically fully developed condition at the inlet of the duct is broken up due to curvature. It is also found that the maximum value of u/u_m increases with the increasing θ up to $\theta=75^o$. However, there are two maximum value of u/u_m as of $\theta=45^o$ and they move toward side walls. It is deduced that the flow field affected by the curvature.

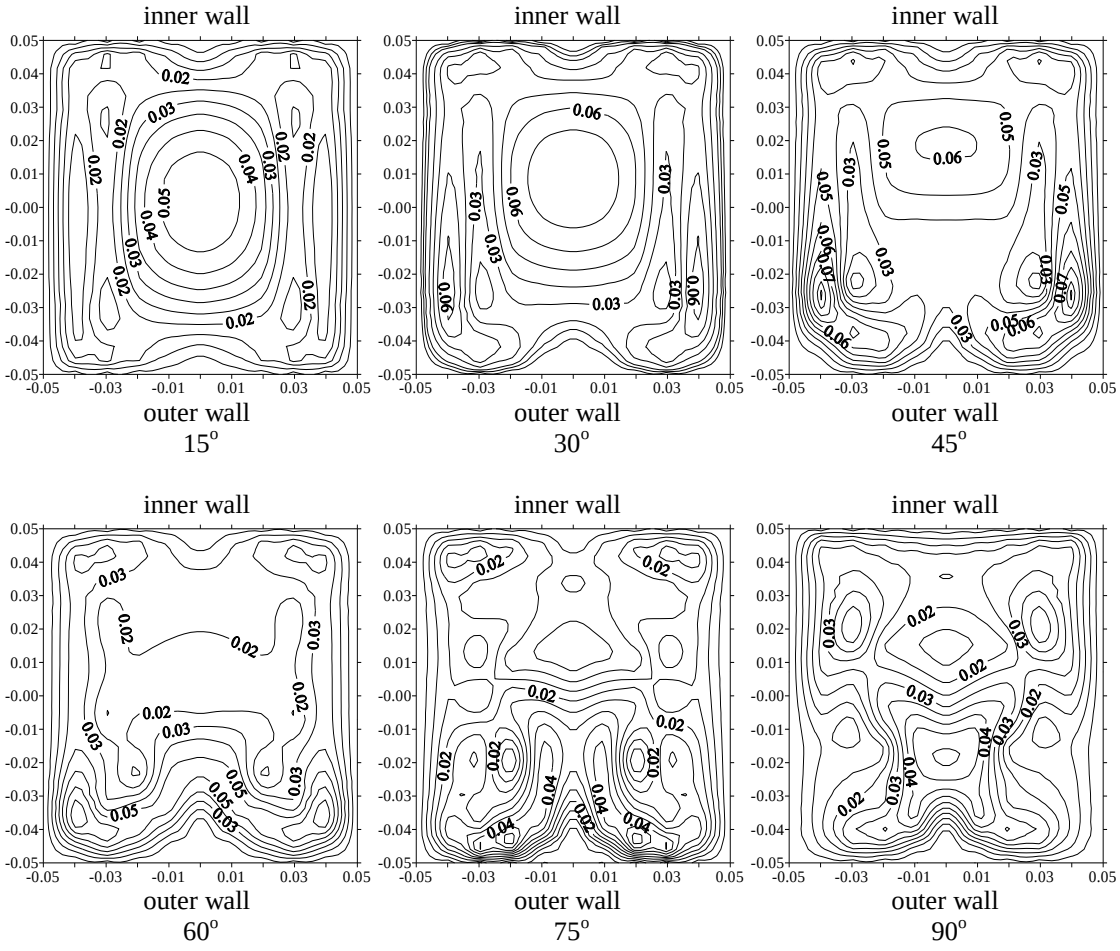

Figure 5 Secondary flow contours at different angles

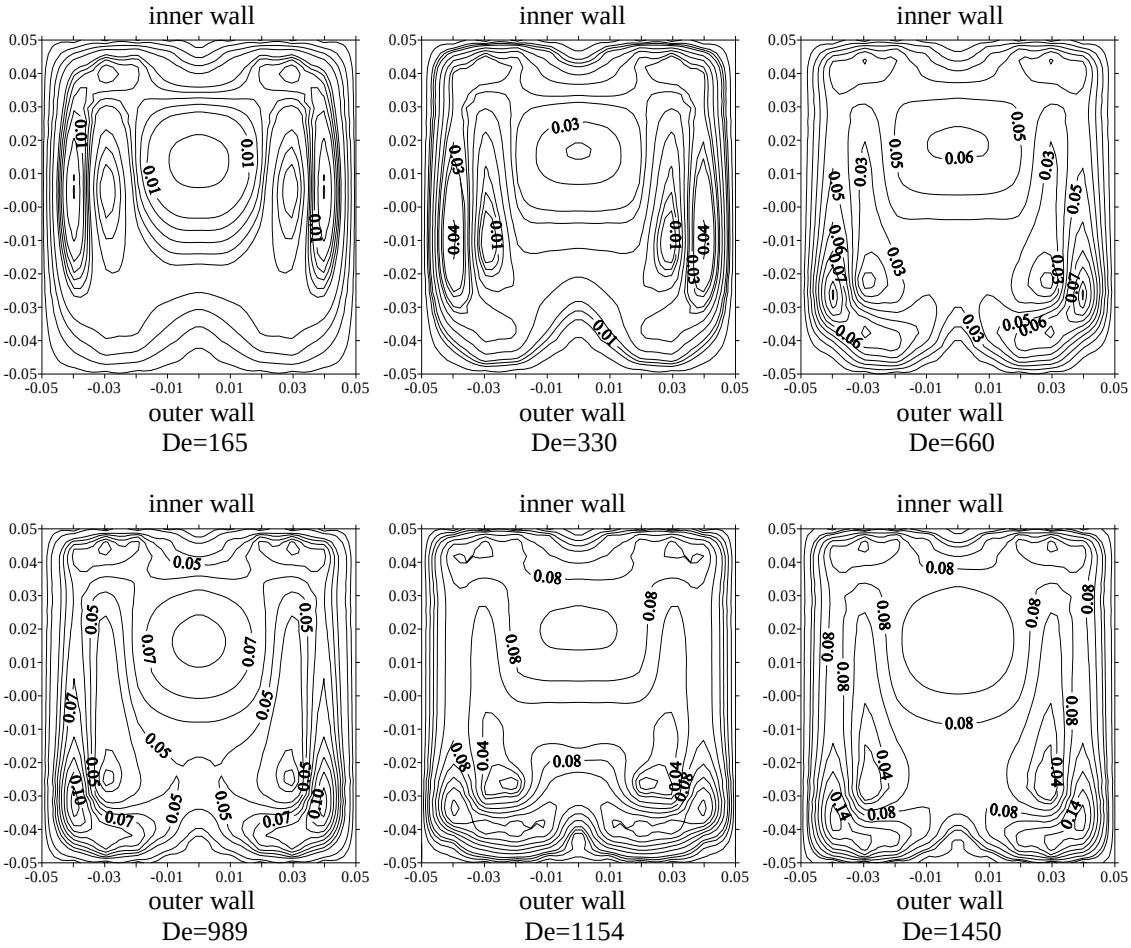

Figure 6 Secondary flow contours on plane created at 45^{o} for different Dean numbers

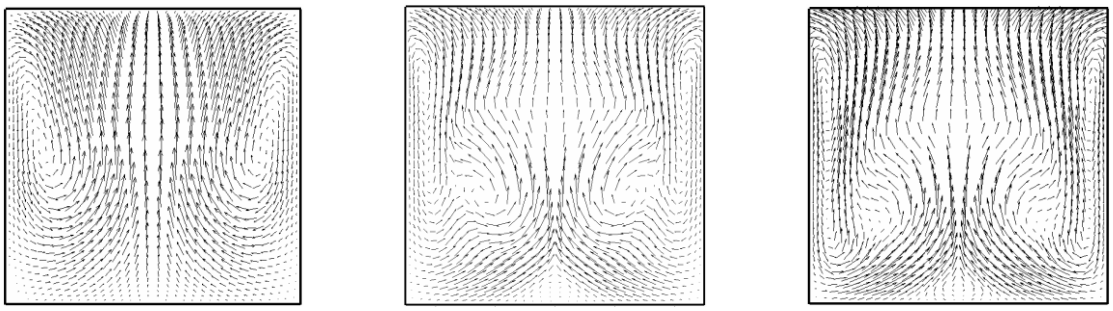

Figure 7. Secondary velocity vectors on outlet plane of the duct for different Dean numbers

(a) (b)

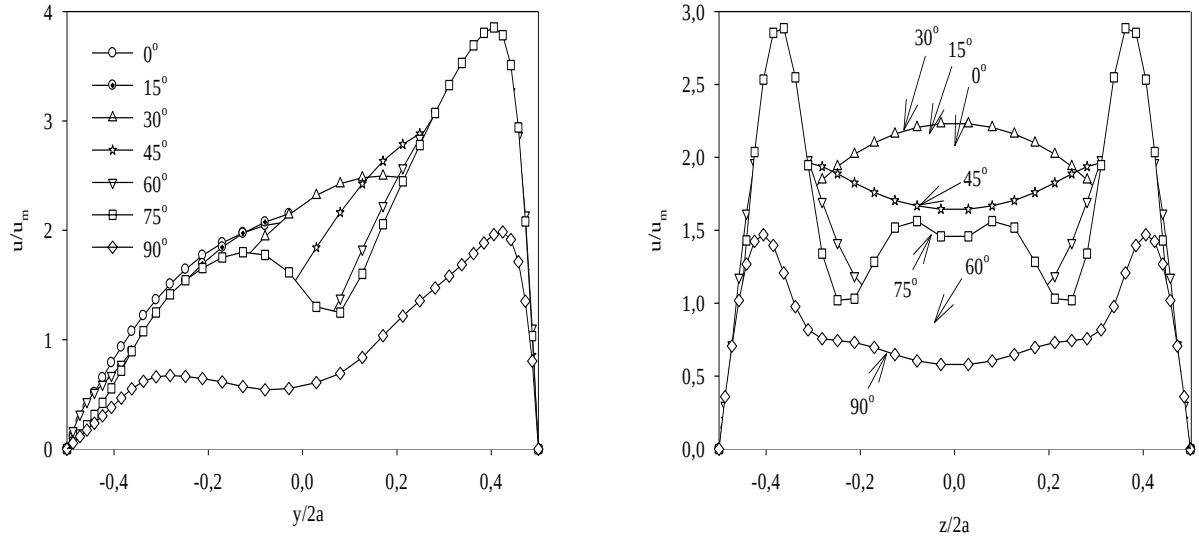

Figure 8. Distribution of u/u_m at z=0 (symmetry plane) (a) and y=0 (b)

In order to determine if thermally fully developed flow has been reached, the peripherally averaged local Nusselt number along the channel is sketched for different Dean numbers in Figure 9. As is shown in the figure, larger Dean number gives larger Nusselt number. It is also seen that local Nusselt number at low Dean number reaches the asymptotic value. In other words, flow reaches the thermally fully developed conditions at the outlet of the duct for low Dean numbers. In addition, it may be deduced that a square curved duct with 90^o is not sufficient to reach fully developed conditions because of small channel radius of curvature at R_c/D_h=2.3 for high Dean numbers. It is seen that the local Nusselt numbers are affected by the secondary flows at the duct cross-section. It is also seen that oscillatory Nusselt number behavior is seen when Dean number is large. The phenomenon is similar to that observed by Cheng et al. (1975), Yee et al. (1980), Chilukuri and Humphrey (1981), Chung and Hyun (1992), and Papadopoulos and Hatzikonstantinou (2005). After 15^o, the secondary flow effect dominates and the local Nusselt number begins to increase until maximum value is reached.

In Figure 10, results for the Nusselt number for fully developed conditions are compared against those of Hwang and Chao (1991), Silva et al. (1999), Papadopoulos and Hatzikonstantinou (2005) and Cheng et al. (1975). Examination of this figure indicates that present results are in good agreement with the literature results. As will be seen in figure, the difference between the results of present and Silva et al. (1999) increases with increasing Dean number. This difference can be from different curvature ratios. As can be seen in figure, heat transfer increases with the increasing Dean number due to the secondary flow.

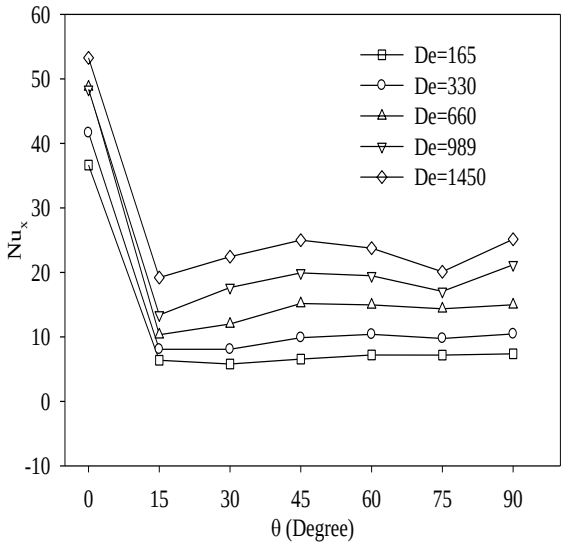

Figure 9 Local Nusselt number along the curved duct for different Dean numbers

Nusselt number for fully developed laminar flow in a straight square duct is 2.98 for constant wall temperature boundary condition (Incropera and DeWitt, 2002). Hence, curved duct results for fully developed condition are compared with the straight square duct result. It is seen that heat transfer in curved channel is higher than the straight duct because of the presence of the secondary field. For example, heat transfer for the square curved duct is approximately five times of the straight square duct for Reynolds number of 1000.

Averaged Nusselt number in the channel is presented as a function of Dean number in Figure 11. As can be seen from figure, Nusselt number increases while the Dean number increases.

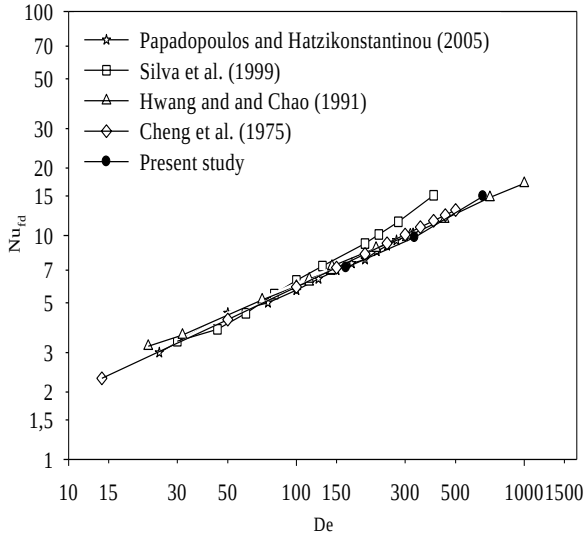

Figure 10 Comparison of fully developed Nusselt number as a function of Dean number

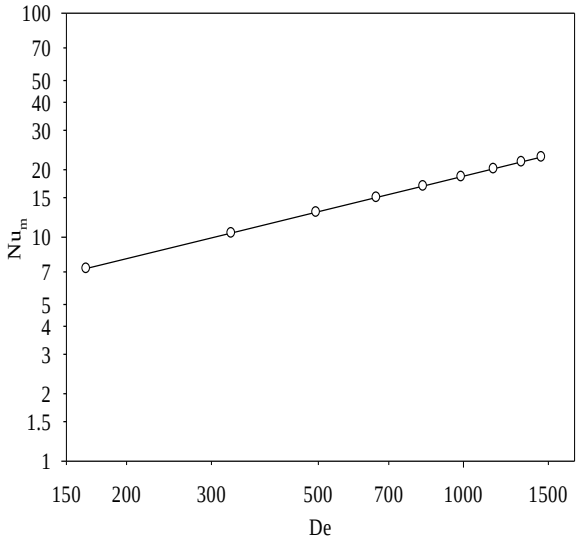

Figure 11 Comparison of the average Nusselt number as a function of Dean number

Based on the three-dimensional study, new engineering correlation is presented in the Eq. (20) for the average Nusselt number as a function of Dean number.

$$Nu_m = 0.4911De^{0.5270} \quad (20)$$

Eq. (20) is valid for the Dean number from 165 to 1450.

The effect of the Dean number on the local friction factor along the duct is shown in Figure 12. It is seen that the friction factor decreases while the Dean number increases. In addition, it is seen that the local friction factors are affected by the secondary flow at the duct cross-section. It is also seen that hydrodynamically fully developed conditions at the inlet of the duct are broken up and flow begins to develop again along the curved duct. It is shown that flow does not reach hydrodynamically fully developed conditions in the channel again. In other words, the radius of curvature in this study is not large enough compared to the channel dimension. This result agrees with the Humphrey et al. (1977). They state that flow does not reach hydrodynamically fully developed conditions in a 90° curved duct with a square cross section for the curvature of 2.3 the same with the present study.

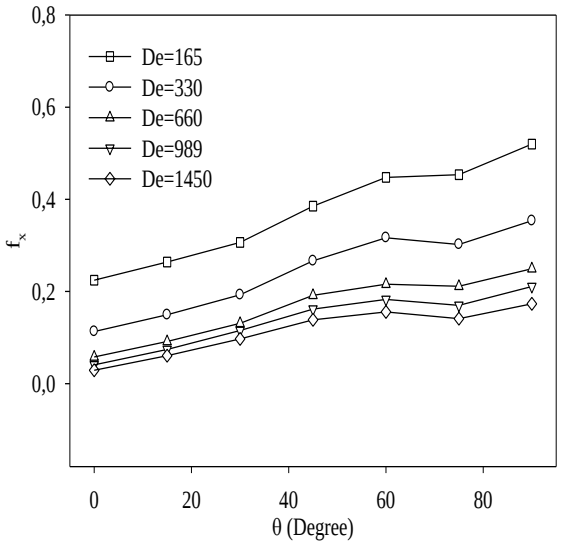

Figure 12 Local Darcy friction factor along the curved duct for different Dean numbers

The curved channel averaged friction factor is presented as a function of Dean number in Figure 13. It is seen that friction factor decreases with the increasing Dean number as a result of the secondary flow.

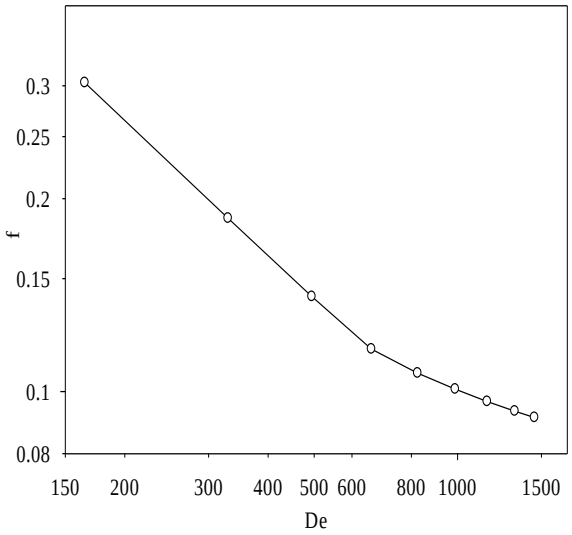

Figure 13 Average Darcy friction factor as a function of Dean number

The average Darcy friction factor is given as below:

$$f = 6.6640De^{-0.6101} \quad (21)$$

This equation is valid for the Dean number between 165 and 1450.

CONCLUSIONS

The present study provides numerical data and correlation for heat transfer and friction factor of laminar flow in a curved duct having a constant square cross section with an aspect ratio of unity and a curvature ratio of 2.3 for constant wall temperature boundary condition. The effects of the Dean number and the curvature of the geometry on the average heat transfer coefficients, the average Darcy friction factors, velocity and temperature are presented. Although flow enters the curved duct at the hydrodynamically fully developed condition, it begins to break up immediately because of the curvature; it is seen that flow does not reach fully developed conditions in the duct again. In addition, it is seen that a curved square duct with 90^o bend angle is not sufficient to reach thermally fully developed flow conditions at low curvature $R_c/2a=2.3$ for large Dean numbers while it is adequate for low Dean numbers. It is shown that the temperature and velocity fields, Nusselt numbers and friction factor are directly affected by secondary flows resulting from centrifugal forces. It has been found that the centrifugal body forces in the curved duct increases the average Darcy friction factor and average Nusselt number. A numerical correlation for average Nusselt number and average Darcy friction factor is obtained in curved duct. It is found that the heat transfer rate in curved square duct is higher than the straight square duct. Results obtained in this study are compared with the literature results and it is found that they are in good agreement.

REFERENCES

Ansys Fluent Inc. Fluent 6.3.26, *User Manuals*, 2006.

Bara, B., Nandakumar, K. and Masliyah, J. H., An Experimental and Numerical Study of the Dean Problem: Flow Development Towards Two-Dimensional Multiple Solutions, *J. Fluid Mech.* 244, 339-376, 1992.

Berger, S. A., Talbor, L. and Yao, L. S., Flow in Curved Pipes, *Annu. Rev. Fluid Mech.* 35, 462-512, 1983.

Cheng, K. C., Lin, R. C. and Ou, J. W., Graetz Problem in Curved Square Channels, *Trans. ASME J. Heat Transfer* 97, 244-248, 1975.

Chilukuri, R. and Humphrey, J. A. C., Numerical Computations of Buoyancy Induced Recirculation in Curved Square Duct Laminar Flow, *Int. J. Heat Mass Trans.* 24, 305-314, 1981.

Chung, J. H. and Hyun, J. M., Convective Heat Transfer in the Developing Flow Region of a Square Duct With Strong Curvature, *Int. J. Heat Mass Trans.* 35, 2537-2550, 1992.

Freitas, C. J., The Issue of Numerical Uncertainity, *Proc. 2nd Int. Conference on CFD in the Minerals and Process Industries*, CDIRO, Melbourne, Australia, 1999.

Hille, P., Vehrenkamp, R. and Schulz-Dubois, E. O., The Development and Structure of Primary and Secondary Flow in a Curved Square Duct, *J. Fluid Mech.* 151, 219-241, 1985.

Humphrey, J. A. C., Taylor, A. M. K. and Whitelaw, J. H., Laminar Flow in a Square Duct of Strong Curvature, *J. Fluid Mech.* 83, 509-527, 1977.

Hwang, G. J. H. and Chao C. H., Forced Laminar Convection in a Curved Isothermal Square Duct, *Trans. ASME J. Heat Transf.* 113, 48-55, 1991.

Incropera, F. P. and DeWitt, D. P., *Fundamentals of Heat and Mass Transfer* (Fifth Ed.), John Wiley & Sons, 2002.

Ito, H., Flow in Curved Pipes, *JSME* 30, 543-552, 1987.

Mori, Y., Uchida, Y. and Ukon, T., Forced Convective Heat Transfer in a Curved Channel With a Square Cross Section, *Int. J. Heat Mass Transf.* 14, 1787-1805, 1971.

Naphon, P. and Wongwises, S., A Review of Flow and Heat Transfer Characteristics in Curved Tubes, *Renew. Sust. Energy Rev.* 10, 463-490, 2006.

Papadopoulos, P. K. and Hatzikonstantinou, P. M., Numerical Analysis of Fully Developed Flow in Curved Square Ducts With Internal Fins, *Trans. ASME J. Fluids Eng.* 126, 752-757, 2004.

Papadopoulos, P. K. and Hatzikonstantinou, P. M., Thermally Developing Flow in Curved Square Ducts With Internal Fins, *Heat Mass Transf.* 42, 30-38, 2005.

Patankar, S. V., *Numerical Heat Transfer and Fluid Flow*, Hemishere Publishing Company, New York, 1980.

Silva, R. J., Valle, R. M. and Ziviani, M., Numerical Hydrodynamic and Thermal Analysis of Laminar Flow in Curved Elliptic and Rectangular Ducts, *Int. J. Therm. Sci.* 38, 585-594, 1999.

Soh, W. Y., Developing Fluid Flow in a Curved Duct of Square Cross-Section and its Fully Developed Dual Solutions, *J. Fluid Mech.* 188, 337-361, 1988.

Versteeg, H. K. and Malalasekra, W., *An Introduction to Computational Fluid Dynamics* (Second Ed.), Prentice Hall, New York, 2007.

Ward-Simith, A. J., *Internal Fluid Flow*, The Fluid Dynamics of Flow in Pipes and Ducts, Clarendon Press, Oxford, 1980.

White, F. M., *Viscous Fluid Flow* (Third Ed.), McGraw Hill, New York, 2006.

Winters, K. H., A Bifurcation Study of Laminar Flow in a Curved Tube of Rectangular Cross-Section, *J. Fluid Mech.* 180, 343-369, 1987.

Yanase, S., Kaga, Y. and Daikai, R., Laminar Flows Through a Curved Rectangular Duct Over a Wide Range of the Aspect Ratio, *Fluid Dynamics Research* 31, 151-183, 2002.

Yee, G., Chilukuri, R. and Humphrey, J. A. C., Developing Flow and Heat Transfer in Strongly Curved Ducts of Rectangular Cross Section, *Trans. ASME J. Heat Transf.* 102, 285-291, 1980.